

1 Proceedings

2 FORTLS: an R Package for Processing TLS data and 3 Estimating Stand Variables in Forest Inventories

4 Juan Alberto Molina-Valero¹, Maria José Ginzo Villamayor², Manuel Antonio Novo Pérez³, Juan
5 Gabriel Álvarez-González¹, Fernando Montes⁴, Adela Martínez-Calvo¹ and César Pérez
6 Cruzado^{5,*}

7 ¹ Unidad de Gestión Ambiental y Forestal Sostenible (UXAFORES), Departamento de Ingeniería
8 Agroforestal, Escuela Politécnica Superior de Ingeniería, Universidade de Santiago de Compostela,
9 Benigno Ledo s/n, Campus Terra, 27002, Lugo, Spain; juanalberto.molina.valero@usc.es;
10 juangabriel.alvarez@usc.es; adela.martinez.calvo@usc.es

11 ² Departamento de Estadística, Análisis Matemático y Optimización, Universidade de Santiago de
12 Compostela, Facultad de Matemáticas, Rúa Lope Gómez de Marzoa s/n. Campus Vida. Santiago de
13 Compostela, Spain. C.P. 15782; mariajose.ginzo@usc.es

14 ³ Instituto Tecnológico de Matemática Industrial (ITMATI), Edificio Instituto Investigaciones Tecnológicas,
15 planta-1. Rúa de Constantino Candeira s/n. Campus Vida. Santiago de Compostela, Spain. C.P.15782;
16 manuelantonio.novo.perez@usc.es

17 ⁴ INIA-Centro de Investigación Forestal, Ctra. De la Coruña km 7,5, 28040 Madrid; fmontes@inia.es

18 ⁵ Unidad de Gestión Ambiental y Forestal Sostenible (UXAFORES), Departamento de Producción Vegetal y
19 Proyectos de Ingeniería, Escuela Politécnica Superior de Ingeniería, Universidade de Santiago de
20 Compostela, Benigno Ledo s/n, Campus Terra, 27002, Lugo, Spain; cesar.cruzado@usc.es

21 * Correspondence: Correspondence: cesar.cruzado@usc.es

22 Published: 25 October 2020

23 **Abstract:** Terrestrial Laser Scanning (TLS) enables rapid, automatic and detailed 3D representation
24 of surfaces with an easily handled scanner device. TLS therefore shows great potential for use in
25 Forest Inventories (FIs). However, the lack of well established algorithms for TLS data processing
26 hampers operational use of the scanner for FI purposes. Here we present FORTLS, an R package
27 specifically developed to automate TLS point cloud data processing for forestry purposes. The
28 FORTLS package enables (i) detection of trees and estimation of their diameter at breast height (*dbh*),
29 (ii) estimation of some stand variables (e.g. density, basal area, mean and dominant height), (iii)
30 computation of metrics related to important tree attributes estimated in FIs at stand level and (iv)
31 optimization of plot design for combining TLS data and field measured data. FORTLS can be used
32 with single-scan TLS data, thus improving data acquisition and shortening the processing time, as
33 well as increasing sample size in a cost-efficient manner. The package also includes several features
34 for correcting occlusion problems in order to produce improved estimates of stand variables. These
35 features of the FORTLS package will enable the operational use of TLS in FIs, in combination with
36 inference techniques derived from model-based and model-assisted approaches.

37 **Keywords:** Forest inventory; LiDAR; remote sensing; R-package; software; stand-level; TLS.

38 1. Introduction

39 Information about forest resources is essential for sustainable forest management and
40 development of forest policies. In this regard, forest inventories (FIs) are used as the main approach
41 to estimating and monitoring the state and evolution of the main variables of interest. FIs have
42 improved since they were first introduced, as a result of the continuous appearance of new
43 technologies, such as Terrestrial Laser Scanning (TLS), considered of great potential value for
44 enhancing FIs [1-2]. However, TLS has not been yet adopted in FIs for several reasons [3], although
45 many studies agree that affordability is the main key challenge to overcome, emphasizing that

46 automation of the point cloud processing with attainable and easy-to-use software able to extract
47 information related to important forest attributes is essential [1-5].

48 As TLS data sets comprise millions of points, sophisticated methods for automatic processing
49 are necessary. In this respect, many algorithms with a high level of automation and that are able to
50 extract tree attributes (diameter at breast height, *dbh*, height, volume, etc.) have been developed in
51 the last few decades [6]. Some of these algorithms have also been included in software applications,
52 e.g. SimpleTree [7], 3D Forest [8] and AutoStem™ [9]. However, there are some drawbacks to using
53 these applications in FIs: (i) single-tree instead of stand-level approaches (SimpleTree); (ii)
54 semiautomatic processing (3D Forest); and (iii) commerciality (not suitable for all users)
55 (AutoStem™).

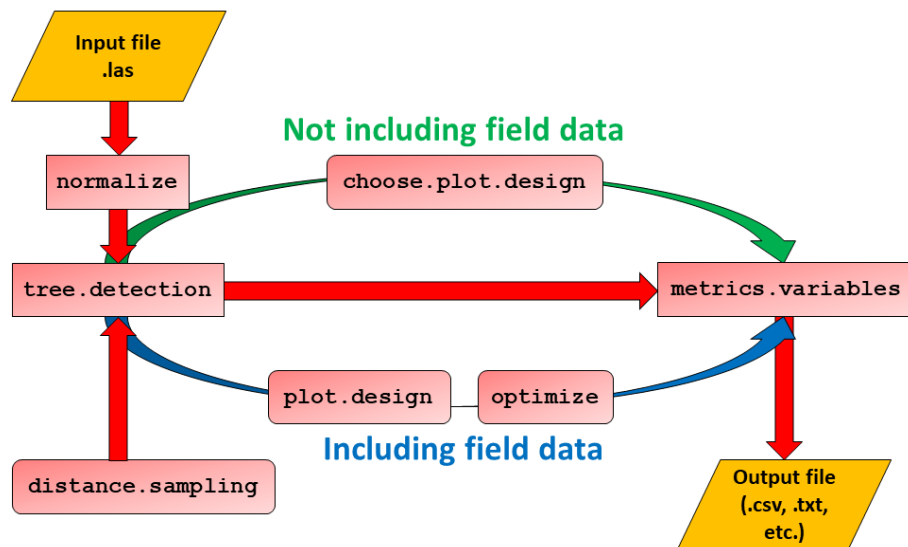
56 Here we present FORTLS, an R package developed with the objective of automating TLS point
57 cloud data processing and estimating variables for forestry purposes. FORTLS can be used with
58 single-scan TLS data and enables (i) detection of trees and estimation of *dbh*, (ii) estimation of some
59 stand variables, such as density (N , trees ha⁻¹), basal area (G , m² ha⁻¹) and mean and dominant height,
60 defined as the mean height of the 100 largest trees ha⁻¹ (h_m and H_0 respectively), (iii) computation of
61 metrics related to important tree attributes estimated in FIs at stand level, and (iv) optimization of
62 plot design for combining TLS data and field measured data. These features of the FORTLS package
63 will enable the operational use of TLS in FIs, in combination with model-based or model-assisted
64 inference approaches.

65 2. Materials and Methods

66 The steps involved in the TLS data processing algorithms are described in the following sections.

67 2.1. Detection of trees and estimation of *dbh*

68 This first algorithm detects trees and estimates their *dbh*, which is the basis for further
69 computations. This is done by the `normalize` function (Figure 1), which obtains coordinates relative
70 to the plot centre and the digital terrain model. This function also applies the point cropping process
71 as a criterion for reducing point density homogeneously in space and proportional to object size [10].
72 The output generated is then used as input for the `tree.detection` function, which detects as
73 many trees as possible from point clouds in the TLS scans. In addition, for every tree detected, the
74 function calculates the coordinates of the section centre, estimates *dbh*, and classifies it as fully visible
75 or partially occluded. Finally, this function obtains the number of points corresponding to 1.3 m
76 height sections of trees (i.e. the *dbh*) for original and reduced point clouds (by applying point cropping
77 process), as well as their estimations.



78

79

80 **Figure 1.** Schematic workflow of FORTLS. The pathway shown in red represents the shortest possible
 81 procedure for estimating variables and metrics. The pathway shown in green includes
 82 `choose.plot.design` as a previous step for assessing the stability of estimations, based only on
 83 TLS data. The pathway shown in blue includes `plot.design` and `optimize` functions with the
 84 objective of determining the best plot design according to field measured data. `distance.sampling`
 is an optional function which can be used in both approaches.

85

2.2. Computation of variables and metrics related to attributes estimated in FIs at stand level

86

87 Once trees have been detected, the next application of FORTLS is to compute variables and
 88 metrics at plot level. For this purpose, the `metrics.variables` function produces a set of TLS-
 89 based variables and metrics related to forest attributes. These can be obtained for different plot
 90 designs (circular fixed area, k-tree and angle-count) if specified in the arguments. This function also
 91 includes features for correcting occlusion problems generated in TLS point clouds. These features are
 92 based on correcting the shadowing effect [11] and gap probability attenuation with distance to TLS
 93 [12]. Apart from these features, others based on distance sampling methods can be applied with the
 94 `distance.sampling` function by implementing point transects methods with the trees detected
 95 [13]. This calculates the detection probability for every tree by fitting probability detection functions
 96 to the histogram of trees distribution according to their distance from plot centre. As in previous
 97 studies by the same authors [13], half normal and hazard rate probability functions without and with
dbh as covariate were used.

98

99 Before using the `metrics.variables` function, previous steps are recommended in order to
 100 select the most appropriate values for the radius, k-tree and BAF (Basal Area Factor) in the function
 arguments. This can be done with or without field data.

101

2.2.1. Field measurements not available

102

103 In this case, the `choose.plot.design` function can be used to plot empirical charts of *N* and
 104 *G* estimates as a function of the plot size (estimation-size charts) for different plot designs (circular
 105 fixed area, k-tree and angle-count), through continuous size increments (radius, k and BAF
 106 respectively). These size-estimation charts represent the consistency in predicting the stand variables
 107 across different values of radius, k and BAF. Size-estimation charts can be drawn for individual
 108 sample plots (including all plots together in the same charts) or for mean values (global mean
 computed for all the sample plots, or for group means if different strata are considered). Finally,

109 different plot designs can be compared if specified in the arguments, producing one size-estimation
 110 chart per variable (*N* and *G*).

111 *2.2.2. Field measurements available*

112 When field measurements are available for the same positions of TLS single-scans, the
 113 `plot.design` and `optimize` functions can be used to assess the performance of TLS-based metrics
 114 and variables relative to field measurements. The `plot.design` function examines correlations
 115 (Pearson and Spearman) and the relative deviance between TLS-based estimates and field
 116 measurements, through plots with continuous size increment. This is done for different plot designs
 117 and by default for the most common metrics and variables, although other metrics/variables may be
 118 considered in the arguments. In a second step, those metrics and variables most closely correlated
 119 with the variables of interest are evaluated by the `optimize` function. This function generates
 120 heatmaps (one per plot design) in which correlations between TLS metrics-variables and estimations
 121 of variables based on field data can be evaluated for all variables and plot sizes.

122 **3. Results**

123 The outputs of the above-mentioned functions are reported below.

124 *3.1. Detection of trees and estimation of their dbh*

125 The result of these applications is a list of the trees detected with the aforementioned
 126 `tree.detection` function, which is a data frame object containing attributes for every tree
 127 detected (Table 1).

128 **Table 1.** Data frame with detected trees and their estimated attributes.

id	file	tree	x	y	phi	phi.lef t	phi.rig ht	dbh	horizontal.dista nce
numeric or character	character (id.txt)	numeric (n)	numeric (m)	numeric (m)		numeric (rad)			numeric (m)
num.points	num.points.est	num.points.hom	num.points.hom.est	partial.occlusion					
numeric (n)				numeric (0-1)					

129
 130 id: identification assigned to a sample plot and which coincides with the file name. file: file name,
 131 consisting of the id and the respective extension (.txt, .csv, etc.). tree: number assigned to every
 132 detected tree (1, 2, ..., n). x: x coordinate of tree centre relative to plot centre. y: y coordinate of tree
 133 centre relative to plot centre. phi: azimuth of tree centre from plot centre. phi.left: azimuth
 134 corresponding to left border of tree section detected. phi.right: azimuth corresponding to right border
 135 of detected tree section. dbh: estimated diameter at breast height. horizontal.distance: horizontal
 136 distance from sample plot centre to tree centre. num.points: number of points corresponding to
 137 normal tree section (1.3 ± 0.05 m). num.points.est: estimated number of points corresponding to
 138 normal tree section (1.3 ± 0.05 m). num.points.hom: number of points corresponding to normal tree
 139 section (1.3 ± 0.05 m) after point cropping process. num.points.est: estimated number of points
 140 corresponding to normal tree section (1.3 ± 0.05 m) after point cropping process. partial.occlusion: tree
 141 fully visible (0) or partial occluded (1).

142 *3.2. Computation of variables and metrics related to attributes estimated in FIs at stand level*

143 The output of the function `metrics.variables` is a list with three data frames, one per plot
 144 design (circular fixed area, k-tree and angle-count plot), containing the following metrics and
 145 variables computed from TLS data:

146 **Table 2.** Structure of list containing metrics and variables.

	<i>N</i>	<i>G</i>	<i>V</i>	<i>dbh_m</i>	<i>dbh_o</i>	Number of points belonging to normal sections	Percentiles
fix.plot	<i>N</i> <i>N.hn</i> ¹ <i>N.hr</i> ¹	<i>G</i> <i>G.hn</i> ¹ <i>G.hr</i> ¹	<i>V</i> <i>V.hn</i> ¹ <i>V.hr</i> ¹	<i>dbh.arit</i> <i>dbh.sqr</i> <i>t</i>	<i>dbh.dom.ari</i> <i>t</i> <i>dbh.dom.sq</i>	<i>num.points</i> <i>num.points.est</i> <i>num.points.ho</i>	<i>P</i> ₁ , <i>P</i> ₅ , <i>P</i> ₁₀ , <i>P</i> ₂₀ , <i>P</i> ₂₅ , <i>P</i> ₃₀ , <i>P</i> ₄₀ ,
k.tree	<i>N.hn.co</i> <i>v</i> ¹	<i>G.hn.co</i> <i>v</i> ¹	<i>V.hn.co</i> <i>v</i> ¹	<i>dbh.geo</i> <i>m</i>	<i>dbh.dom.ge</i> <i>om</i>	<i>num.points.ho</i> <i>m</i> <i>num.points.ho</i>	<i>P</i> ₅₀ , <i>P</i> ₆₀ , <i>P</i> ₇₀ , <i>P</i> ₇₅ ,
angle.count	<i>N.hr.co</i> <i>v</i> ¹ <i>N.sh</i> ¹ <i>N.corr</i> ²	<i>G.hr.co</i> <i>v</i> ¹ <i>G.sh</i> ¹ <i>G.corr</i> ²	<i>V.hr.co</i> <i>v</i> ¹ <i>V.sh</i> ¹ <i>V.corr</i> ²	<i>dbh.har</i> <i>m</i>	<i>dbh.dom.ha</i> <i>rm</i>	<i>m</i> <i>m.est</i>	<i>P</i> ₈₀ , <i>P</i> ₉₀ , <i>P</i> ₉₅ , <i>P</i> ₉₉

147 *N*: all *N* variables are direct estimates of *N*, estimated using trees detected in TLS data. They are
 148 computed without considering occlusion corrections (*N*) and by implementing distance sampling
 149 methodologies (*N.hn*, *N.hr*, *N.hn.cov*, *N.hr.cov*), shadowing effect (*N.sh*) and gap probability
 150 attenuation with distance from TLS (*N.corr*). *G*: all *G* variables are direct estimates of *G*, estimated
 151 using detected trees from TLS data. They are computed without considering occlusion corrections (*G*)
 152 and by implementing distance sampling methodologies (*G.hn*, *G.hr*, *G.hn.cov*, *G.hr.cov*), shadowing
 153 effect (*G.sh*) and gap probability attenuation with distance from TLS (*G.corr*). *V*: all *V* variables are
 154 direct estimates of *V*, estimated using trees detected in TLS data. They are computed without
 155 considering occlusion corrections (*V*) and by implementing distance sampling methodologies (*V.hn*,
 156 *V.hr*, *V.hn.cov*, *V.hr.cov*), shadowing effect (*V.sh*) and gap probability attenuation with distance from
 157 TLS (*V.corr*). *dbh_m*: estimated *dbh* mean for detected trees using arithmetic (*dbh.arit*), square
 158 (*dbh.sqr*), geometric (*dbh.geom*) and harmonic means (*dbh.har*). *dbh_o*: estimated dominant *dbh*
 159 mean (considering the 100 largest trees ha⁻¹) for trees detected using arithmetic (*dbh.dom.ari*), square
 160 (*dbh.dom.sqr*), geometric (*dbh.dom.geom*) and harmonic means (*dbh.dom.har*). Number of points
 161 belonging to normal sections: sum of points belonging to normal sections of all trees detected from
 162 the original point cloud (*num.points*) and reduced point cloud, reduced using point cropping process
 163 (*num.points.ho*), and number of points estimated from the original point cloud (*num.points.est*)
 164 and reduced point cloud, reduced using the point cropping process (*num.points.ho.est*). Percentiles:
 165 percentile of *z* coordinate (*m*) relative to ground level.

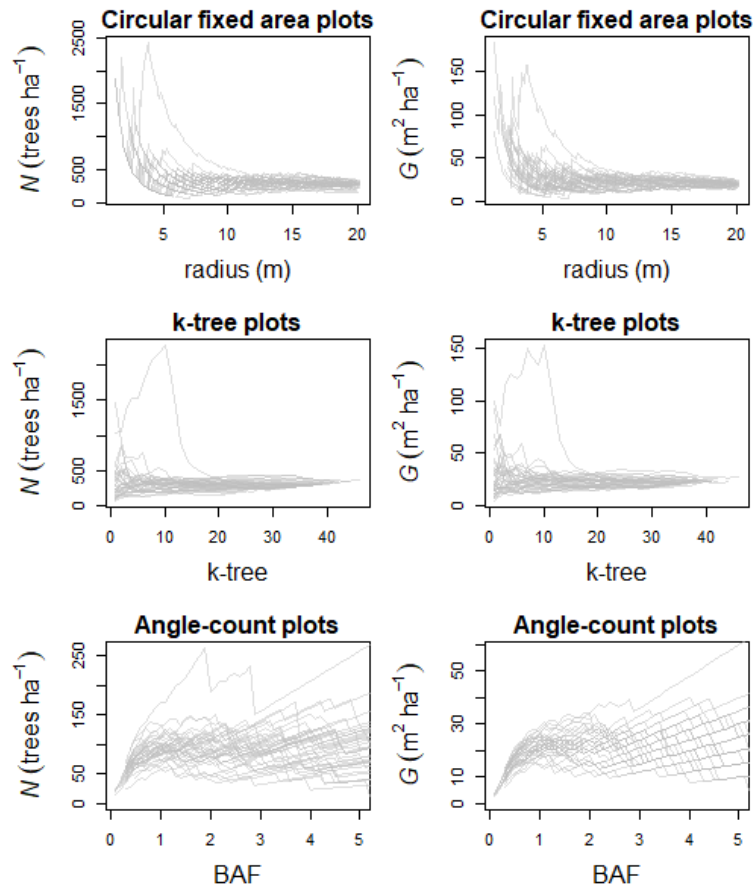
166 ¹ Variables are just computed for fix area and k-tree plots.

167 ² Variables are just computed for angle count plots.

168

169 3.2.1. Plot design when field measurements are not available

170 Figure 2 is an example of `choose.plot.design` output when no arguments are defined. In
 171 these graphical representations, it can be observed that estimations of *N* and *G* become approximately
 172 stable from a radius of 8 m (circular fixed area plot) and 10 trees (k-tree plot) and at between 1 and 2
 173 for BAF (angle count plot).



174

175

176

177

Figure 2. Line charts with estimated values of N and G for different plot designs (circular fixed area, k-tree and angle-count), through continuous size increments (radius, k and BAF respectively). Each grey line represents a sample plot.

178

3.2.2. Plot design when field measurements are available

179

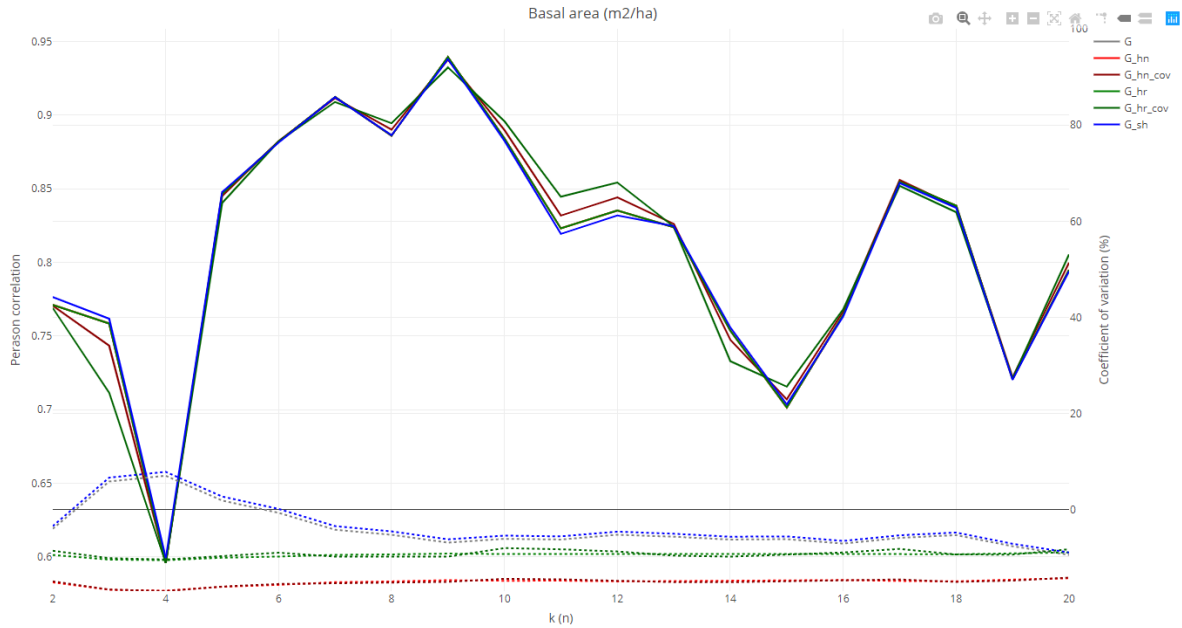
180

181

182

183

The outputs of the `plot.design` function are line charts showing correlation patterns and relative deviance for TLS derived metrics-variables and estimations of variables based on field data, for different designs and sizes of plots. One interactive chart (html file) per plot design (circular fixed area, k-tree and angle-count plot) and variables of interest (N , G , V , h_m , H_0 , dbh_m , dbh_0) (Figure 3), as well as their associated database as (csv file), are saved in the work directory.



184

185

186

187 **Figure 3.** Line chart showing Pearson correlation (continuous line) and relative deviance (dotted line)
188 for basal area estimation based on field data and the TLS derived metrics and variables: G (direct
189 estimates of G estimated using trees detected in TLS data), G_hn, G_hr, G_hn.cov, G_hr.cov (considering
190 occlusion corrections based on distance sampling methodologies) and G_sh (considering occlusion
191 corrections based on shadowing effect) through continuous size increment (k) for the k-tree plot design.

192

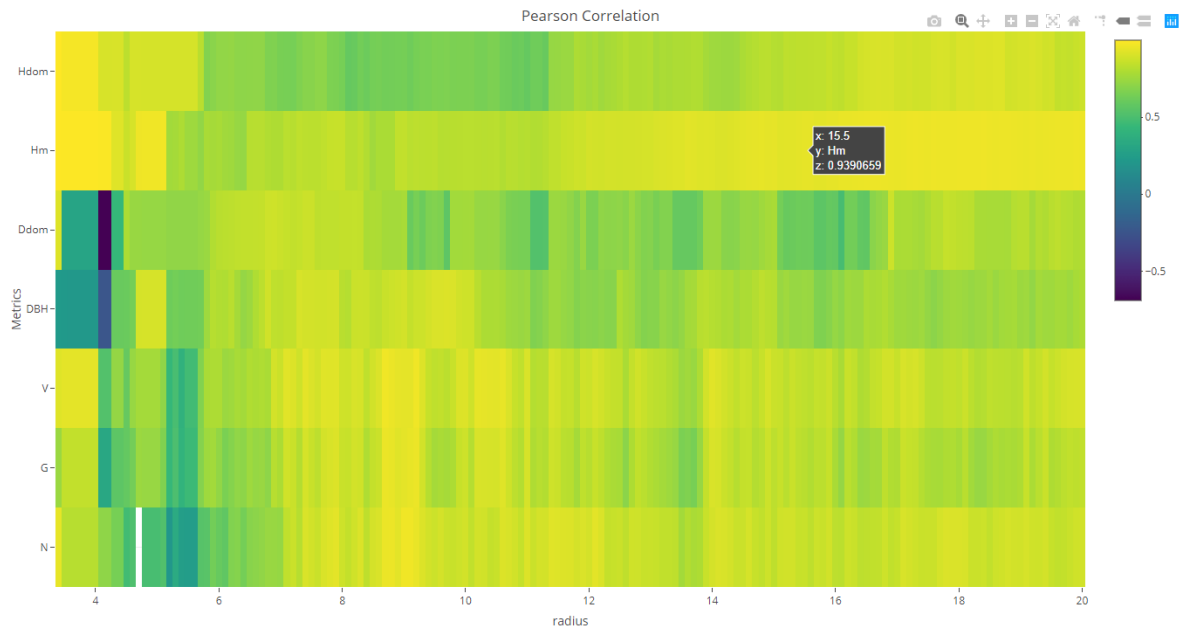
193

194

195

196

Once all TLS metrics and variables have been assessed according to how they are correlated with the variables of interest, the next step is to evaluate them with the `optimize` function. This function generates interactive heatmaps (one per plot design) in which the behaviour of those metrics showing the best correlations across continuous plot size increment can be observed (Figure 4). The color palette gives warm and cold colours to highly positive and negative correlations respectively.



197

198

Figure 4. Heatmap showing correlations between variables of interest and TLS variables-metrics.

199 4. Discussion

200 FORTLS enables automated processing of TLS point clouds and production of variables and
201 metrics related to relevant information about forest attributes. As some of the functions assess the
202 performance of variable estimations for different plot designs, the application finds the best possible
203 sampling design for any case. This attribute makes FORTLS a flexible application for FIs purposes
204 and valid for several types of forests.

205 Although FORTLS can be used without including conventional field data, its use is optimal
206 when TLS data and field measured data are combined and assessed with the `plot.design` and
207 `optimize` functions. This enables optimization of plot design by assessing correlations between
208 variables of interest (*dbh*, *H*, *G*, etc.) and metrics and variables computed for TLS data, which enables
209 selection of the most appropriate plot designs for each situation. In the best case, those metrics and
210 variables for which low deviations from field measurements are obtained can be used to estimate
211 variables, as in other conventional methods. However, occlusions caused by trees, especially in
212 single-scan data, represent the main problem in this approach [3]. This drawback may be solved with
213 some of the occlusion correction features implemented in this package, as assessed in previous
214 studies [11-13].

215 The utility of the R package FORTLS for operational use of TLS in FIs has been demonstrated,
216 confirming previous conclusions considered a guideline for further research on TLS in forestry [5].
217 As FORTLS works with single-scan data, co-registration of point clouds in specific software and
218 placement of targets at field measurements are not required. This improves data acquisition and
219 shortens the processing time, as well as increasing sample size in a cost-efficient manner, which is
220 one of the most desirable features of TLS in FIs [3]. Further research with study cases and considering
221 different metrics that are potentially highly correlated with forest attributes is necessary in order to
222 consolidate this R package.

223 **Funding:** This research was funded by Spanish Ministry of Science, Innovation and Universities, AGL2016-
224 76769-C2-2-R. JAMV was funded by the Spanish Ministry of Education through the FPU program
225 (FPU16/03057).

226 **Acknowledgments:** The authors thank Mario López Fernández for help with fieldwork.

227 References

- 228 1. Dassot, M.; Constant, T.; Fournier, M. The use of terrestrial LiDAR technology in forest science: application
229 fields, benefits and challenges. *Annals of forest science* **2011**, *68*(5), 959-974.
- 230 2. White, J. C.; Coops, N. C.; Wulder, M. A.; Vastaranta, M.; Hilker, T.; Tompalski, P. Remote sensing
231 technologies for enhancing forest inventories: A review. *Canadian Journal of Remote Sensing*, **2016**, *42*(5), 619-
232 641. <https://doi.org/10.1080/07038992.2016.1207484>
- 233 3. Liang, X.; Kankare, V.; Hyyppä, J.; Wang, Y.; Kukko, A.; Haggrén, H.; ... Holopainen, M. Terrestrial laser
234 scanning in forest inventories. *ISPRS Journal of Photogrammetry and Remote Sensing* **2016**, *115*, 63-77.
235 <https://doi.org/10.1016/j.isprsjprs.2016.01.006>
- 236 4. Newnham, G. J.; Armston, J. D.; Calders, K.; Disney, M. I.; Lovell, J. L.; Schaaf, C. B.; ... Danson, F. M.
237 Terrestrial laser scanning for plot-scale forest measurement. *Current Forestry Reports* **2015**, *1*(4), 239-251.
- 238 5. Liang, X.; Kukko, A.; Hyyppä, J.; Lehtomäki, M.; Pyörälä, J.; Yu, X.; ... Wang, Y. In-situ measurements from
239 mobile platforms: An emerging approach to address the old challenges associated with forest inventories.
240 *ISPRS Journal of Photogrammetry and Remote Sensing*, **2018**, *143*, 97-107.
241 <https://doi.org/10.1016/j.isprsjprs.2018.04.019>
- 242 6. Liang, X.; Hyyppä, J.; Kaartinen, H.; Lehtomäki, M.; Pyörälä, J.; Pfeifer, N.; ... Huang, H. International
243 benchmarking of terrestrial laser scanning approaches for forest inventories. *ISPRS journal of*
244 *photogrammetry and remote sensing* **2018**, *144*, 137-179. <https://doi.org/10.1016/j.isprsjprs.2018.06.021>
- 245 7. Hackenberg, J., Spiecker, H., Calders, K., Disney, M., & Raunonen, P. (2015). SimpleTree—an efficient open
246 source tool to build tree models from TLS clouds. *Forests*, *6*(11), 4245-4294. <https://doi.org/10.3390/f6114245>

- 247 8. Trochta, J., Krůček, M., Vrška, T., & Král, K. (2017). 3D Forest: An application for descriptions of three-
248 dimensional forest structures using terrestrial LiDAR. *PloS one*, 12(5).
249 <https://doi/10.1371/journal.pone.0176871>
- 250 9. Bienert, A., Scheller, S., Keane, E., Mohan, F., & Nugent, C., 2007. Tree detection and diameter estimations
251 by analysis of forest terrestrial lasers canner point clouds. In *ISPRS workshop on laser scanning* (Vol. 36, pp.
252 50-55).
- 253 10. Molina Valero, J. A., Ginzo Villamayor, M. J., Novo Pérez, M. A., Álvarez-González, J. G., Pérez-Cruzado,
254 C. 2019. Estimación del área basimétrica en masas maduras de *Pinus sylvestris* en base a una única medición
255 del escáner láser terrestre (TLS). *Cuadernos de la Sociedad Española de Ciencias Forestales* 45(3): 97-116.
256 DOI: 10.31167/csecfv0i45.19887
- 257 11. Seidel, D., & Ammer, C. (2014). Efficient measurements of basal area in short rotation forests based on
258 terrestrial laser scanning under special consideration of shadowing. *iForest-Biogeosciences and Forestry*, 7(4),
259 227. <https://doi.org/10.3832/ifor1084-007>
- 260 12. Strahler, A. H., Jupp, D. L., Woodcock, C. E., Schaaf, C. B., Yao, T., Zhao, F., ... & Ni-Miester, W. (2008).
261 Retrieval of forest structural parameters using a ground-based lidar instrument (Echidna®). *Canadian*
262 *Journal of Remote Sensing*, 34(sup2), S426-S440. <https://doi.org/10.5589/m08-046>
- 263 13. Astrup, R., Ducey, M. J., Granhus, A., Ritter, T., & von Lüpke, N. (2014). Approaches for estimating stand-
264 level volume using terrestrial laser scanning in a single-scan mode. *Canadian Journal of Forest Research*, 44(6),
265 666-676. <https://doi.org/10.1139/cjfr-2013-0535>
- 266
267
268

269